Available online at www.sciencedirect.com
SCIENCE DIRECT®
Journal of Solid State Chemistry 178 (2005) 2927–2933
JOURNAL OF SOLID STATE CHEMISTRY
www.elsevier.com/locate/jssc

Phase transition, thermal expansion and electrical properties of $BiCu_2VO_6$

Ivana Radosavljević Evans[a,*], Shanwen Tao[b], John T.S. Irvine[b]

[a]Department of Chemistry, University of Durham, Science Site, South Road, Durham DH1 3LE, England, UK
[b]School of Chemistry, University of St. Andrews, Fife KY16 9ST, Scotland, UK

Received 6 June 2005; received in revised form 1 July 2005; accepted 8 July 2005

Abstract

Phase transition in $BiCu_2VO_6$ has been studied by variable temperature powder and single crystal X-ray diffraction. A reversible single-crystal-to-single-crystal phase transition has been identified and the high-temperature β-$BiCu_2VO_6$ polymorph structurally characterized. β-$BiCu_2VO_6$ is monoclinic I-centered and related to the α-form by a subgroup–supergroup relationship. Bi atoms are coordinated to oxygen so as to give rise to $(BiO_2)^-$ chains parallel to the c-axis. The magnetic Cu–O sublattice forms a complex system of quasi one-dimensional ladders, built up by five- and six-coordinate Cu atoms. Dynamic disorder in the high temperature structure can be described in terms of librational motion of VO_4 tetrahedral group. AC impedance measurements suggest predominantly electronic conduction in this material.

Keywords: Phase transitions

1. Introduction

Ternary mixed bismuth oxides of general formula BiA_2MO_6 (M = Cu, Mg, Zn, Mn, Cd, Ca, Pb; A = P, As, V) adopt closely related crystal structures. They all consist of $(BiO_2)^-$ infinite chains, $(MO_4)^{3-}$ tetrahedra and interspersed A^{2+} cations, and the differences in the exact arrangement of these building blocks give rise to the variations on the basic structure type. At room temperatures, most of these phases are primitive orthorhombic, with unit cell edges of about 5, 8 and 12 Å. Phase transitions to higher symmetry structures have been detected in $BiMg_2VO_6$, $BiPb_2VO_6$, $BiMg_2PO_6$ and $BiZn_2PO_6$ [1–4], although only in the first two cases have the high temperature forms been fully structurally characterized.

$BiCu_2VO_6$ was first prepared and reported in 1998 [5]. At room temperature it is primitive monoclinic in space group $P2_1/n$ and this structure will hereinafter be referred to as α-$BiCu_2VO_6$. It was subsequently found that this phase possesses interesting magnetic properties, as it has a non-magnetic singlet ground state and a gap in the spin excitation spectrum [6]. In this paper, we present a variable temperature diffraction study of $BiCu_2VO_6$ and show that a reversible phase transition occurs in this material at about 450 K. The crystal structure of the high-temperature form, β-$BiCu_2VO_6$, is also presented. Electrical conductivity has been investigated by AC impedance spectroscopy of pressed pellets.

2. Experimental

A polycrystalline sample of $BiCu_2VO_6$ was synthesized by the solid-state reaction of Bi_2O_3 (Atomergic Chemetals, 99.9%), CuO (Cerac, 99.9%) and NH_4VO_3 (Johnson Matthey, 99.99%). Stoichiometric quantities of the reagents were ground and heated in an alumina crucible at 750 °C for 20 h. Single crystal growth was

*Corresponding author. Fax: +44 191 384 4737.
E-mail address: ivana.radosavljevic@durham.ac.uk (I.R. Evans).

0022-4596/$ - see front matter © 2005 Elsevier Inc. All rights reserved.
doi:10.1016/j.jssc.2005.07.006

carried out by melting a small amount of the polycrystalline sample at 1000 °C, slow cooling it to 600 °C at a rate of 3 °C/h and then to room temperature at a rate of 5 °C/min. Dark brown crystals of elongated prismatic shape were obtained. The chemical composition of several crystals was analyzed using an SX-50 electron microprobe. The results confirmed the Bi:Cu:V ratio of 1:2:1.

Variable temperature powder X-ray diffraction data were collected using a Bruker AXS D8 Advance diffractometer equipped with an Anton Paar HTK1200 high-temperature stage. Starting from 30 °C, a data collection was performed every 10° on heating to 700 °C and on cooling down to 30 °C. The heating rate between temperatures was 0.5°/s, 2θ range between 10° and 90°, step size 0.0144° and step time 0.3 s, resulting in a data collection time of 28 min per temperature. A small amount of Al_2O_3 was added to the sample as an internal standard for temperature calibration.

A single crystal of $BiCu_2VO_6$ with approximate dimensions of $0.04 \times 0.08 \times 0.26\,mm^3$ was selected for data collection. The data were collected using a Bruker AXS SMART diffractometer with a CCD detector and Mo$K\alpha$ radiation, equipped with an Oxford Cryosystems nitrogen Cryostream Plus temperature control system. Data were collected at 120, 300 and 500 K. At each temperature, a full sphere of data was collected with a frame width of 0.3° and a counting time of 30 s/frame. Data reduction was carried out using the SAINT [7] software suite. An absorption correction was applied by face-indexing, followed by a multiscan [8] correction. The crystal structures were solved by direct methods using SIR92 [9] and refined in the Crystals [10] software package. Full crystallographic details are given in Table 1.

The conductivity of $BiCu_2VO_6$ was measured by AC impedance. A Schlumberger Solartron 1260 frequency response analyzer coupled with a 1287 electrochemical interface controlled by *Z*-plot electrochemical impedance software was used over the frequency range 1–100 mHz. The $BiCu_2VO_6$ powder was pressed to pellets under a pressure of 5 tons/cm^2. It was found that the pellets disintegrated after firing at 700 °C for 2 h. Green, unfired, pellets coated with gold electrodes were therefore used for measurements performed in laboratory air.

Table 1
Crystallographic details for $BiCu_2VO_6$

Temperature (K)	120	300	500
Crystal system	Monoclinic	Monoclinic	Monoclinic
Space group	$P2_1/n$	$P2_1/n$	$I2/m$
a (Å)	13.4831(4)	13.5117(4)	13.585(4)
b (Å)	7.8295(2)	7.8363(2)	7.883(2)
c (Å)	15.7983(5)	15.8166(5)	15.963(6)
β (°)	113.141(1)	113.098(1)	112.96(1)
V (Å^3)	1533.57(8)	1540.44(8)	1574.2(8)
Z	12	12	12
Calc. ρ (g/cm^{-3})	6.28	6.25	6.11
μ (mm^{-1})	44.25	44.06	43.11
Total no. of reflections	11614	12295	5144
No. of unique reflections	4056	4242	2113
No. of obs. reflections	3085	3006	1725
No. of par. refined	272	272	156
R_{int} (%)	3.4	3.3	4.8
R (%)	5.26	4.46	5.84
wR (%)	5.98	5.17	6.83

3. Results and discussion

3.1. Phase transition in $BiCu_2VO_6$ and thermal expansion properties

The room temperature structure of $BiCu_2VO_6$ from the literature [5] was used to carry out Rietveld refinements of the 136 variable temperature powder patterns [11].

The only structural parameters refined were the cell parameters and an overall temperature factor for $BiCu_2VO_6$ and the same parameters for the internal standard Al_2O_3. The other parameters refined were sample displacement, twelve background terms and six terms describing a pseudo Voigt profile function. Temperature calibration was performed by correcting the obtained thermal expansion data for alumina on the basis of literature values given by Taylor [12].

The plots of the cell parameters of $BiCu_2VO_6$ as a function of temperature are given in Figs. 1a–e. The dependence of all unit cell parameters on temperature shows a change in slope at about 450 K without a hysteresis, suggesting that a structural phase transition occurs at this temperature both on heating and cooling (Fig. 1). Volume coefficient of thermal expansion changes from $2.70 \times 10^{-5}\,K^{-1}$ below the phase transition to $3.41 \times 10^{-5}\,K^{-1}$ above it.

3.2. Polymorphism in $BiCu_2VO_6$

Structure solution and refinement of the single crystal data collected at 120 and 300 K give results consistent with the previously published model in monoclinic space group $P2_1/n$, with the asymmetric unit consisting of 3Bi, 6Cu, 3V and 18O atoms, all on general positions. However, analysis of the 500 K data set indicated that a cell centering phase transition had occurred and the unit cell parameters obtained were $a = 13.585(4)$ Å, $b = 7.883(2)$ Å, $c = 15.963(6)$ Å, $\beta = 112.96(1)$ and space group $I2/m$. Atomic fractional coordinates are given in Table 2 and two views of the unit cell in Fig. 2.

The β-$BiCu_2VO_6$ structure contains 3Bi, 3Cu, 3V and 13O unique atoms. As in the room temperature form, all Cu atoms are on general positions, but Bi and V have moved onto mirror planes. Out of 13 independent oxygen atoms, five remain on general sites, while six

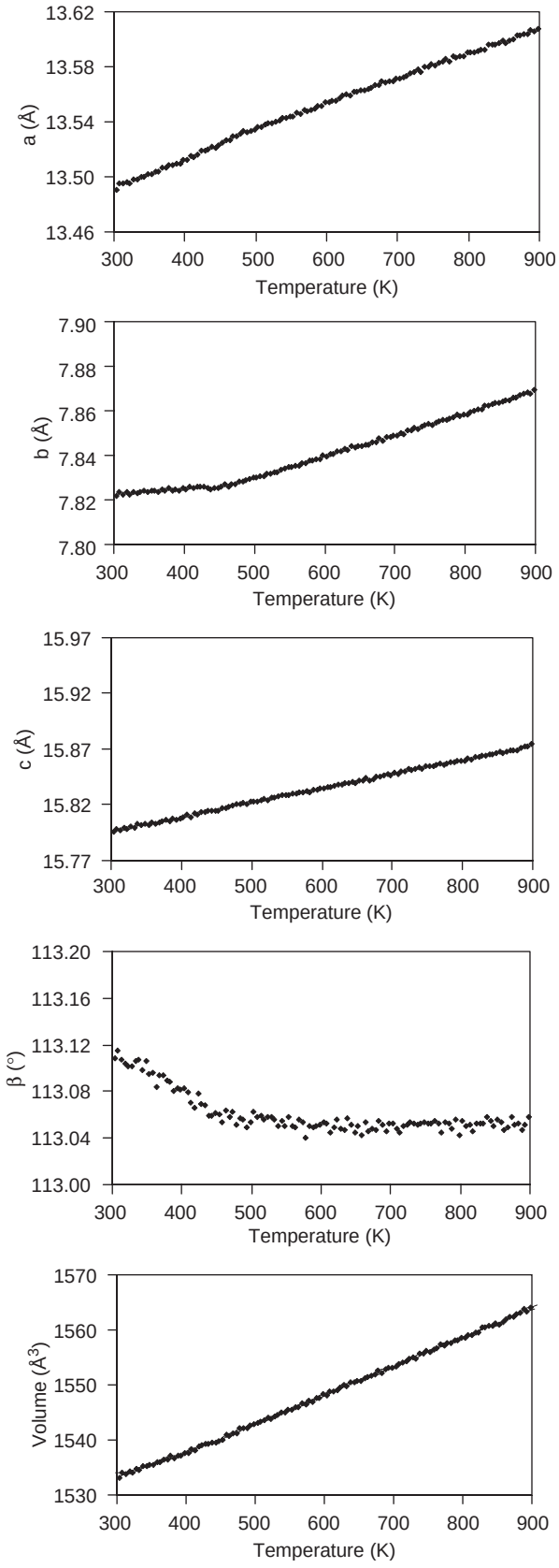

Fig. 1. Variation of the unit cell parameters of $BiCu_2VO_6$ as a function of temperature (a, b and c plotted using a constant percentage change scale on the *y*-axes). Both heating and cooling stages are plotted.

Table 2
Fractional atomic coordinates for β-$BiCu_2VO_6$ at 500 K

Atom	*x*	*y*	*z*	*U*eq. (Å^2)
Bi(1)	0.87905(5)	–0.5	−0.28754(4)	0.0169
Bi(2)	1.08782(5)	–0.5	−0.38049(4)	0.0157
Bi(3)	1.09215(5)	–0.5	−0.06095(5)	0.0165
Cu(4)	0.91954(12)	–0.1808(2)	−0.10287(10)	0.0156
Cu(5)	1.06193(14)	–0.2015(2)	−0.23638(11)	0.0214
Cu(6)	0.91774(14)	–0.1844(2)	−0.44552(10)	0.0176
V(7)	1.1898(2)	0	−0.0401(2)	0.0222
V(8)	1.1924(2)	0	−0.34622(19)	0.0137
V(9)	0.8087(2)	0	−0.3154(2)	0.0184
O(10)	0.9857(6)	–0.3239(12)	−0.1708(5)	0.0166
O(11)	1	–0.6744(14)	−0.5	0.012
O(12)	1.1073(11)	0	−0.1599(9)	0.0212
O(13)	1	–0.6741(15)	0	0.0143
O(14)	0.9066(13)	0	−0.3633(10)	0.0235
O(15)	0.9731(7)	–0.3384(11)	−0.3424(5)	0.0165
O(16)	0.8772(13)	0	−0.5336(9)	0.0279
O(17)	1.1525(8)	–0.1735(13)	−0.3048(6)	0.0236
O(18)	1.1708(10)	–0.5	−0.1861(10)	0.0295
O(19)	0.8870(11)	0	−0.0268(10)	0.0262
O(20)	0.8708(11)	0	−0.1944(9)	0.0204
O(21)	0.7621(17)	–0.329(3)	−0.5211(10)	0.111
O(22)	0.7618(14)	–0.323(3)	−0.1533(10)	0.0824

have moved onto mirror planes and two onto two-fold axes. The coordination environment of Bi in β-$BiCu_2VO_6$ is similar to that in the α-form. All three Bi atoms have four short bonds to oxygens (2.2–2.3 Å), forming BiO_4 rectangular pyramids that share edges, giving rise to $(BiO_2)^-$ chains parallel to the *c* crystallographic axis (Fig. 3). One of the unique Bi atoms, however, has an additional bonded oxygen, O(18) at 2.6 Å.

There are three unique Cu atoms in two different types of coordination environments. Two Cu atoms are five-coordinate. They form distorted square pyramids that share edges to form Cu_2O_8 dimers, which then share two corners to form Cu_4O_{14} quadrimers. In both cases there are four shorter Cu–O bonds (1.95–2.00 Å), while the fifth is longer (2.27–2.28 Å). The third Cu atom is in a distorted octahedral geometry, with four shorter bonds between 1.95 and 1.99 Å, and two longer ones of 2.73 and 2.78 Å. Pairs of distorted edge-sharing octahedra (Cu_2O_{10}) link up with Cu_4O_{14} units to form a ladder running along the crystallographic *c*-direction. Cu–O ladders are separated by Bi^{3+} and V^{5+} cations, but they are also connected by corner sharing of Cu_2O_{10} units, so that every third copper atom in each ladder provides a link to the adjacent ladder via a Cu–O–Cu bridge (Fig. 4).

This type of connectivity is essentially the same as in α-$BiCu_2VO_6$, but with slightly higher symmetry. Instead of 12, there are eight unique Cu–O–Cu bonds within each ladder, giving rise to a complex pathway for magnetic interactions. $BiCu_2VO_6$ has recently been

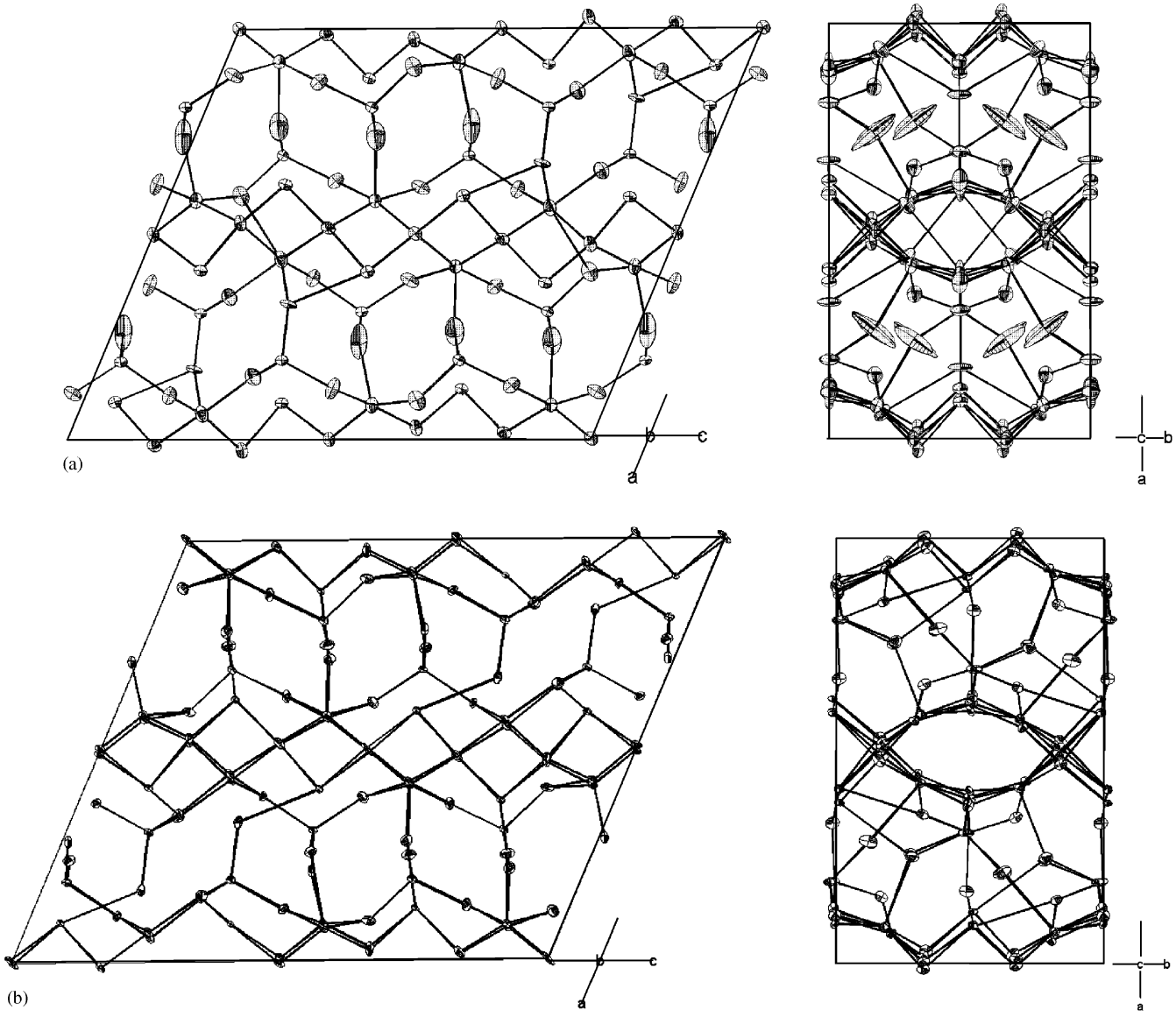

Fig. 2. Two views of the crystal structure of $BiCu_2VO_6$ at (a) 500 K and (b) 120 K. Thermal ellipsoids are shown at the 50% probability level.

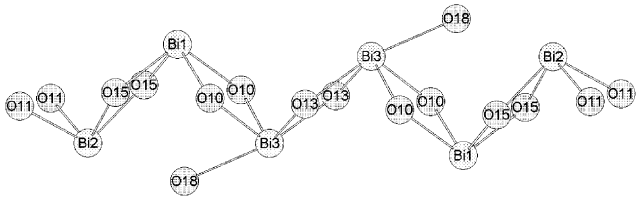

Fig. 3. Coordination environment of Bi atoms in β-$BiCu_2VO_6$ and formation of $(BiO_2)^-$ chains.

identified as a narrow band spin gap material [6], but the exact model of the magnetic interactions (quasi one dimensional ladder vs. interacting dimers) has not been established from the neutron inelastic scattering experiments on the polycrystalline sample, due to the inherent structural complexity of this phase.

As in the room temperature form, the three unique V atoms in β-$BiCu_2VO_6$ are in tetrahedral coordination. Fig. 5 and data in Table 2 show that two oxygen atoms, O(21) and O(22), in VO_4 tetrahedra display large anisotropic atomic displacement parameters (ADPs). TLS analysis [13] has been carried out on this structural model and the results suggest that these ADPs are consistent with librational motion of the VO_4 groups, with the major component about the crystallographic *c*-axis (14°, 6° and 10° for V(7), V(8) and V(9), respectively, Fig. 5). The large ADPs of atoms O(21) and O(22) and different magnitudes of librational motion reflect the different environments of the three

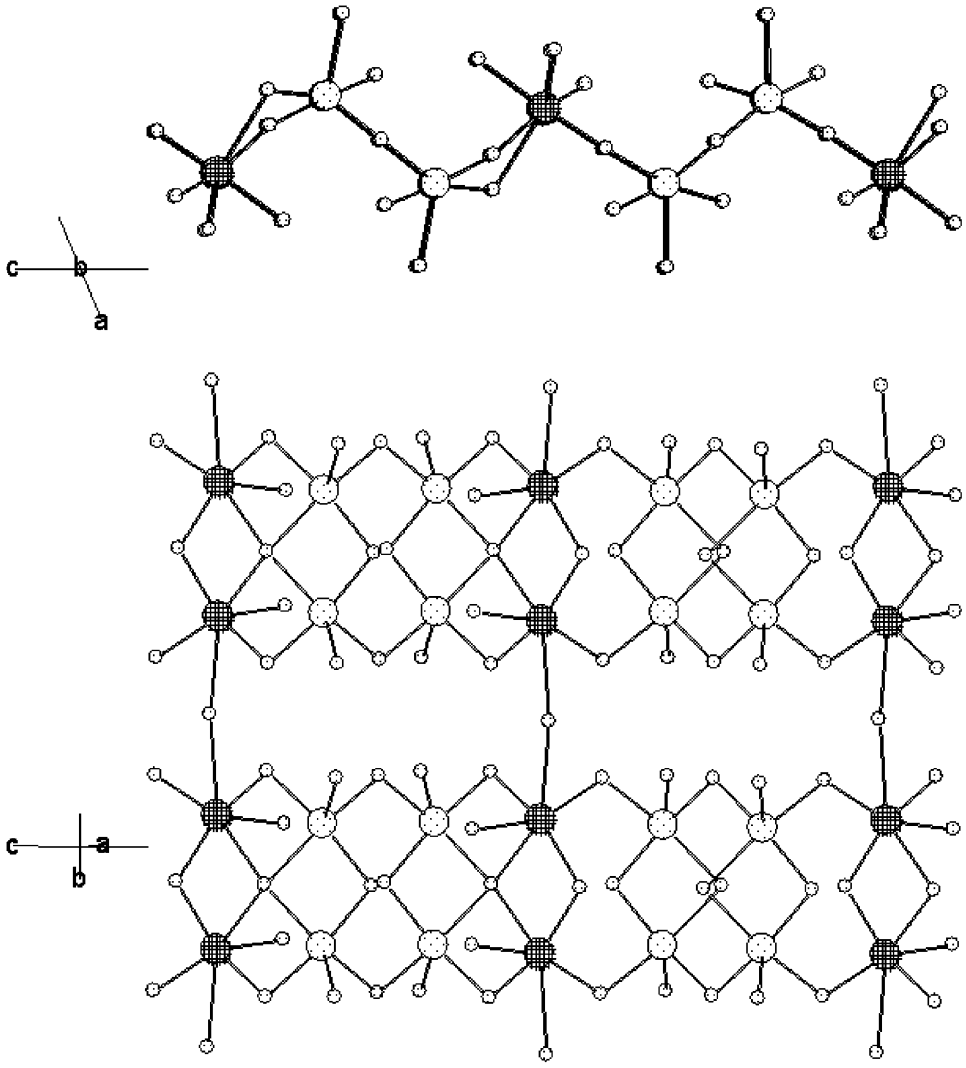

Fig. 4. Two mutually perpendicular views of the Cu–O sublattice in β-$BiCu_2VO_6$: 5-coordinate Cu atoms shown as light dotted circles, 6-coordinate Cu atoms as dark hatched circles, O atoms as small circles. Bi and V atoms have been omitted from this figure for clarity.

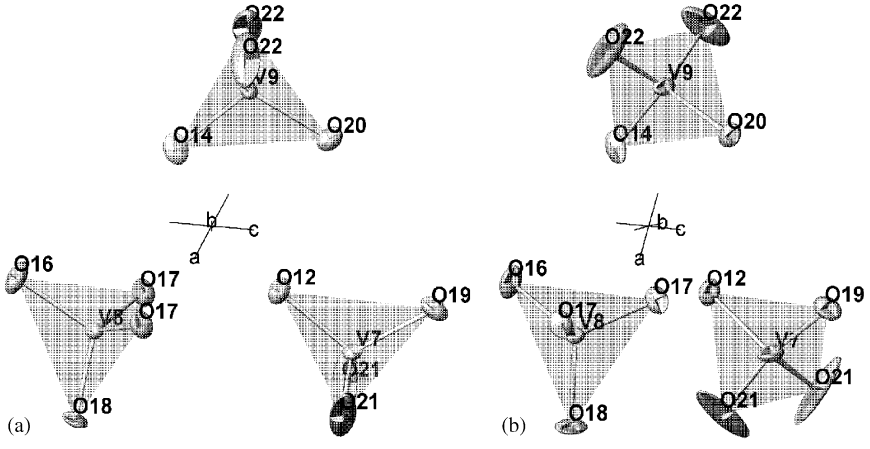

Fig. 5. Two views of the three unique VO_4 groups in β-$BiCu_2VO_6$ with their ADPs.

unique V atoms. V(7) and V(9) bond to oxygen atoms O(21) and O(22), respectively. These are the only two-coordinate oxygen atoms in the structure, bonding only to two five-coordinate Cu atoms, providing a shared corner between the VO_4 and CuO_5 groups. The vanadate group of atom V(8) is different in that all its oxygen atoms are three- or four-coordinate. It is more strongly 'pinned down', there is less freedom for librational motion and the ADPs of its oxygen atoms are smaller than for O(21) and O(22).

An alternative structural model can be postulated in principle, where the dynamic disorder of the VO_4 tetrahedral groups is replaced by static disorder with O(21) and O(22) sites split. The refinement of this model gives the same agreement factors as the former one. However, since the two oxygen atoms with large ADPs are the only two-coordinate oxygens in the structure and the elongation of the thermal ellipsoids is perpendicular to the M–O–M bonds, the dynamically disordered model for the 500 K structure seems plausible.

The dependence of the unit cell parameters of $BiCu_2VO_6$ on temperature and the relationship between the structure of α-$BiCu_2VO_6$ and the β-form suggest that the phase transition is of second order. Temperature cycling experiments also show that this is a reversible single-crystal-to-single-crystal transition.

3.3. Electrical conductivity properties

Two features are observed in the impedance spectrum corresponding to the presence of both bulk and grain boundary elements. A flattened semi-circular arc, is observed in the AC impedance spectrum of $BiCu_2VO_6$, shown in Fig. 6. The lack of low-frequency structure

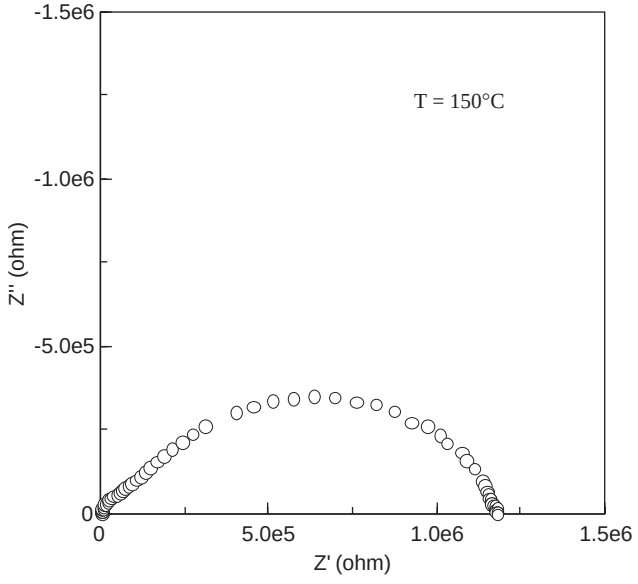

Fig. 6. AC impedance plots, $-Z''$ versus Z', obtained at 150 °C for $BiCu_2VO_6$.

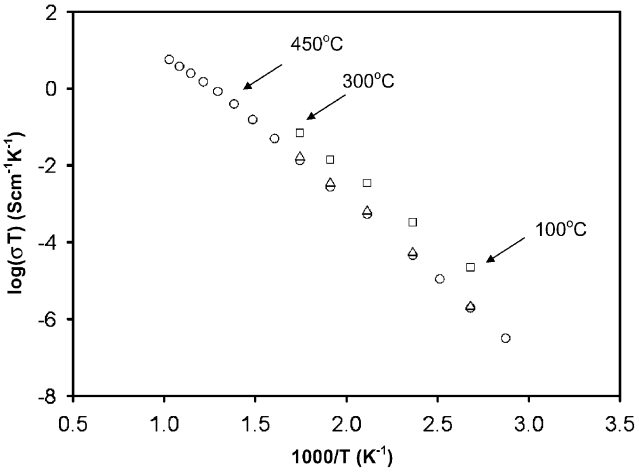

Fig. 7. Conductivity of $BiCu_2VO_6$ as a function of temperature: ○ total, □ bulk, △ grain boundary contribution.

indicates that electronic conduction is dominant. The Arrhenius plot of the total AC conductivity of $BiCu_2VO_6$ as a function of temperature is displayed in Fig. 7. A change of slope is noticeable at about 450 °C, with the calculated activation energies for the total conduction process of 0.81 ± 0.02 eV between 75 and 450 °C, and 0.64 ± 0.02 eV between 450 and 700 °C. In the temperature region between 100 and 300 °C, the bulk and grain boundary resistance could be separated, and the corresponding calculated activation energies are 0.74 ± 0.02 and 0.82 ± 0.02 eV. The total conductivities in air are 5.46×10^{-4} and 5.91×10^{-2} S/cm at 450 and 700 °C, respectively. The change in slope could arise from a number of possible causes: loss of oxygen on heating, decreasing number of carriers, sintering of $BiCu_2VO_6$ to decrease grain boundary contribution or simply changing to a region where the bulk conductivity becomes a dominant feature in the impedance spectrum. The impedance value at these temperatures is too small to allow the component capacitance values to be measured directly at these temperatures. Although there is a small difference between the activation energy for total conductivity at high temperatures and bulk conductivity at low temperatures, it still seems the change in total energy is primarily driven by change from bulk to grain boundary domination. Most probably a certain degree of in situ sintering gives rise to the slight change in activation energy.

Acknowledgments

IRE thanks the EPSRC for the Academic Fellowship. Judith Howard is acknowledged for the provision of single crystal and John Evans for powder X-ray diffraction facilities.

References

[1] I. Radosavljevic, A.W. Sleight, J. Solid State Chem. 149 (2000) 143.
[2] I. Radosavljevic Evans, J.S.O. Evans, J.A.K. Howard, J. Mater. Chem. 12 (9) (2002) 2648.
[3] I. Radosavljevic, J.A.K. Howard, A.W. Sleight, Int. J. Inorg. Mater. 2 (2000) 543.
[4] E.M. Ketatni, B. Memari, F. Abraham, O. Mentre, J. Solid State Chem. 153 (2000) 48.
[5] I. Radosavljevic, J.S.O. Evans, A.W. Sleight, J. Solid State Chem. 141 (1998) 149.
[6] T. Masuda, A. Zheludev, H. Kageyama, A.N. Vasilyev, Europhys. Lett. 63 (5) (2003) 757.
[7] SAINT+, Release 6.22. Bruker Analytical Systems, Madison, Wisconsin, USA, 1997–2001.
[8] G.M. Sheldrick, SADABS, University of Göttingen, Germany, 1998.
[9] A. Altomare, G. Cascarano, C. Giacovazzo, A. Guagliardi, M.C. Burla, G. Polidori, M. Camalli, J. Appl. Cryst. 27 (1994) 435.
[10] P.W. Betteridge, J.R. Carruthers, R.I. Cooper, K. Prout, D.J. Watkin, J. Appl. Cryst. 36 (2003) 1487.
[11] Topas v2.0: General Profile and Structure Analysis Software for Powder Diffraction Data, Bruker AXS, Karlsruhe, Germany, 2000
[12] D. Taylor, Br. Ceram. Trans. J. 83 (4) (1984) 92.
[13] V. Schomaker, K.N. Trueblood, Acta Cryst. B 24 (1968) 63.